On the Green function of the Lord-Shulman thermoelasticity equations

Zhi-Wei Wang,[156] Li-Yun Fu*,[2] Jia Wei,[156] Wanting Hou,[2] Jing Ba[3], José M. Carcione[4]

[1] Key Laboratory of Petroleum Resource Research, Institute of Geology and Geophysics, Chinese Academy of Sciences, Beijing 100029, P. R. China.

[2] Key Laboratory of Deep Oil and Gas, China University of Petroleum (East China), Qingdao 266580, P. R. China.

[3] School of Earth Sciences and Engineering, Hohai University, Nanjing 211100, China.

[4] Istituto Nazionale di Oceanografia e di Geofisica Sperimentale (OGS), Borgo Grotta Gigante 42c, Sgonico, Trieste 34010, Italy

[5] Innovation Academy for Earth Science, CAS, Beijing 100029, P. R. China

[6] University of Chinese Academy of Sciences, Beijing 100049, P. R. China

*Corresponding author. lfu@upc.edu.cn

SUMMARY

Thermoelasticity extends the classical elastic theory by coupling the fields of particle displacement and temperature. The classical theory of thermoelasticity, based on a parabolic-type heat-conduction equation, is characteristic of an unphysical behavior of thermoelastic waves with discontinuities and infinite velocities as a function of frequency. A better physical system of equations incorporates a relaxation term into the heat equation, the equations predict three propagation modes, namely, a fast P wave (E wave), a slow thermal P wave (T wave), and a shear wave (S wave). We formulate a second-order tensor Green's function based on the Fourier transform of the thermodynamic equations. It is the displacement-temperature solution to a point (elastic or heat) source. The snapshots, obtained with the derived second-order tensor Green's function, show that the elastic and thermal P modes are dispersive and lossy, which is confirmed by a plane-wave analysis. These modes have similar characteristics of the fast and slow P waves of poroelasticity. Particularly, the thermal mode is diffusive at low thermal conductivities and becomes wave-like for high thermal conductivities.

Key words: Wave propagation; Fourier analysis; Numerical solutions; Seismic attenuation.

1 INTRODUCTION

Thermoelasticity is an extension of classical elasticity, which deals with the interaction between the displacement and temperature fields (Lord & Shulman 1967; Green & Lindsay 1972; Green & Naghdi 1993; Hetnarski & Ignaczak 1997; Chandrasekharaiah 1998; Tzou 1995). The study of wave propagation in a thermoelastic solid is of fundamental importance in several disciplines such as seismic exploration (Zener 1938; Treitel 1959; Savage 1966; Armstrong 1984), geothermal studies (Jacquey *et al*. 2015) and earthquake seismology (Boschi 1973), and others (Tsai 2011; Auriault 2014). Hetnarski & Ignaczak (1999) explain the difference theories in terms of the input properties and predicted waves.

The theory of thermoelasticity has been established by Biot (1956) on the basis of the thermodynamics of irreversible process. Deresiewicz (1957) applies a plane-wave analysis to investigate propagation of waves in an isotropic thermoelastic solid. Three kinds of waves propagate, namely, E wave, T wave, and S wave. The T wave has been observed in experimental measurements for some specific materials. Ackerman *et al*. (1966) observed it in solid helium, while McNelly *et al*. (1970) and Jackson *et al*. (1970) detected the T wave in NaF crystals. However, the longitudinal E and T waves predicted by Biot and Deresiewicz have infinite velocities at infinite frequencies, since the classical thermoelastic equations are based on a parabolic-type heat transfer equation. This anomalous behavior can be avoided by introducing a relaxation term into the heat equation (e.g., Vernotte 1948; Lord & Shulman 1967; Green & Lindsay 1972; Turchetti & Mainardi 1976; Ignaczak & Ostoja-Starzewski 2010). Banerjee & Pao (1974) investigate the propagation of plane harmonic waves in anisotropic media. Nowacki (1975) constructs the thermodynamic foundation of thermoelasticity systematically and develops the Green function for anisotropic media, based on the classical thermoelasticity equation with the unrealistic infinite velocity. Similarly, Tosaka (1985) derives Green's function for boundary-element analyses based on the same thermoelasticity equation. Rudgers (1990) studies the characteristic of thermoelastic waves as a function of frequency. Norris (1994) describes a procedure to generate

fundamental solutions or the Green functions for time harmonic point forces and sources for the theories of piezoelectricity, thermoelasticity, and poroelasticity. Bear *et al*. (1992) and Sharma (2008) investigate the theory of thermo-poroelasticity. To our knowledge, Carcione *et al.* (2018, 2019) are the first to simulate thermoelastic and thermo-poroelastic wave propagation with realistic propagation velocities, including a relaxation term in the heat equation, i.e., the Lord-Shulman theory and its generalization to the poroelastic case. The algorithm is based on the Fourier pseudospectral method, with the simulations showing the thermal wave and the Biot slow wave.

Many researchers have used Green's function to study wave propagation in elastic or viscoelastic media, but with few studies on the Green function in thermoelastic media. The fundamental solutions for case of isotropic thermoelasticity is known (Kupradze *et al.* 1979). Tosaka & Suh (1991) formulate the Green function based on the classical thermoelastic theory (a parabolic-type heat equation). Here, we obtain the Green function of the thermoelasticity equations with one relaxation time, based on the theory of Lord & Shulman (1967) (a hyperbolic-type heat equation). Fundamental solutions (or Green's functions) play an important role in the numerical solution of partial differential equations by integral equation methods, and as a test of numerical solutions. First, we analyze the characteristic of the wave propagation in thermoelastic media by a plane-wave method, the theory predicts two distinct lossy longitudinal waves, i.e., E wave and T wave, whereas the predicted S wave is unaffected by the thermal effects. Then, we formulate the integral equation of the modified thermoelasticity equations (Hörmander 2013) in the frequency domain and obtain the second-order tensor Green's function corresponding to point loadings (force or heat sources) in a homogeneous isotropic material. Finally, we calculate wavefield snapshots to analyze displacements and temperatures, corresponding to vertical and horizontal loadings (heat sources).

2 EQUATIONS OF THERMOELASTICITY

Biot (1956) and Deresiewicz (1957) establish the relations between stress, strain and temperature in linear isotropic media. However, their equations lack the relaxation term in the heat equation, leading to physically unacceptable solutions for the T wave (i.e., infinite phase velocity). The modified thermoelasticity equations with a relaxation term are (e.g., Carcione *et al*., 2018) are written by using the Einstein implicit

summation as follows.

Strain-displacement relations:

$$\epsilon_{ij} = \frac{1}{2}\left(u_{i,j} + u_{j,i}\right), \tag{1}$$

where u_i and ϵ_{ij} are the components of displacement and strain, respectively.

Stress-strain relations for isotropic media

$$\sigma_{ij} = 2\mu\epsilon_{ij} + \lambda\delta_{ij}u_{k,k} - \beta\delta_{ij}T + f_{ij}, \tag{2}$$

where σ_{ij} are the stress components, λ and μ are the Lamé constants, δ_{ij} are the Kronecker-delta components, f_{ij} are external stress forces, T is the increment of temperature above a reference absolute temperature T_0, and $\beta = (3\lambda+2\mu)\alpha$ with α being the coefficient of thermal expansion. Equation (2) indicates that the temperature-induced elastic variations in stress strongly depend on the coefficient of thermal expansion.

Equations of momentum conservation:

$$\sigma_{ji,j} = \rho\ddot{u}_i + f_i, \tag{3}$$

where f_i are the components of external body forces, ρ is the mass density, and a dot above a variable denotes time differentiation.

Law of hear conduction:

$$\gamma\Delta T = c\left(\dot{T} + \tau\ddot{T}\right) + T_0\beta\left(\dot{u}_{k,k} + \tau\ddot{u}_{k,k}\right) + q, \tag{4}$$

where γ is the coefficient of thermal conductivity, c is the specific heat of the unit volume in the absence of deformation, τ is a relaxation time, q is a heat source, and Δ is the Laplacian operator. The resultant temperature gradient that leads to heat transfer depends not only on the heat source, but also on the strain rate at each point of the elastic body. A relaxation time τ is introduced to make the heat equation hyperbolic, leading to wave-like behavior for the T wave.

By combining equations (1)- (4), we obtain

$$\begin{cases} \mu u_{i,jj} + (\lambda+\mu)u_{j,ji} - \beta T_{,i} = \rho\ddot{u}_i, \\ \gamma T_{,jj} = c\left(\dot{T} + \tau\ddot{T}\right) + T_0\beta\left(\dot{u}_{j,j} + \tau\ddot{u}_{j,j}\right) + q. \end{cases} \tag{5}$$

Equation (5) couples the mechanical and thermal motions. The strain and temperature fields are coupled as a result of the action of elastic and heat sources. S waves are not affected by the temperature, since the shear strain is not coupled with the heat equation. On the other hand, the P wave generates temperature gradients leading to mechanical

energy dissipation and heat-conduction absorption, while the heat equation predicts a T wave analogous to the slow P wave of Biot theory of poroelasticity. In fact, the static constitutive equations of poroelasticity and thermoelasticity are formally the same if we identify the pore-fluid pressure with the temperature and the fluid compression with entropy (Norris 1991).

3 DISPERSION ANALYSES WITH PLANE WAVES

A plane-wave analysis of the thermoelasticity equations provides a simple way to understand the physics of wave propagation in thermoelastic media. Let us consider the following plane-wave expression of the displacement components and temperature fluctuations,

$$\begin{cases} u_i = Ad_i \exp[\mathrm{i}\omega(t - sl_i x_i)], \\ T = B \exp\left[\mathrm{i}\omega\left((t - sl_i x_i)\right)\right], \end{cases} \tag{6}$$

where ω is the angular frequency, t is the time, $s = 1/V_\mathrm{c}$ is the slowness with V_c being the complex velocity, d_i is a unit vector denoting the direction of displacement, x_i is the position components, l_i is the directions defining the propagation direction, A and B are amplitude constants, and i =√(-1).

3.1 Dispersion relations

For the S wave, $d_i\, l_i$=0 (Deresiewicz 1957), that is, the direction of displacement is perpendicular to propagation direction. As formulated in Appendix B, we obtain the following dispersion relation for this wave,

$$\begin{cases} \left[\mu\left(\dfrac{\omega}{V_\mathrm{c}}\right)^2 - \rho\omega^2\right]A - \mathrm{i}\dfrac{\omega}{V_\mathrm{c}}\beta B = 0, \\ \left[\mathrm{i}\omega c - \omega^2\tau + \gamma\left(\dfrac{\omega}{V_\mathrm{c}}\right)^2\right]B = 0. \end{cases} \tag{7}$$

The solution to this equation results in the S wave velocity,

$$B = 0, V_\mathrm{c} = \sqrt{\mu/\rho}. \tag{8}$$

We see that the S wave propagation is lossless because of the isotropic assumption in the current thermoelasticity theory, where the shear stresses are independent of temperature, and therefore they are not coupled with the heat-conduction equation. Likewise, for P waves, $d_i\, l_i$ = 1 (Deresiewicz 1957), that is, the direction of displacement is parallel to the propagation direction. As described in Appendix B, we obtain the

following dispersion relation,

$$\left[-\rho\omega^2 + (\lambda + 2\mu)\left(\frac{\omega}{V_c}\right)^2\right]\left[\mathrm{i}c\omega + \gamma\left(\frac{\omega}{V_c}\right)^2 - c\tau\omega^2\right] = -\beta^2\gamma\, T_0 \frac{\omega}{V_c}(\mathrm{i}\omega - \tau\omega^2). \quad (9)$$

The solution to this equation results in complex velocities for the P waves,

$$2V_c^2 = V_A^2 + M \pm \sqrt{(V_A^2 + M)^2 - 4V_I^2 M}. \quad (10)$$

where $M = \mathrm{i}\omega a^2/(1+\mathrm{i}\omega\tau)$, with $a = \sqrt{(\gamma/c)}$, is a complex kernel arising from a Maxwell mechanical model of viscoelasticity (Carcione 2014), $V_I = \sqrt{((\lambda+2\mu)/\rho)}$ and $V_A = \sqrt{(V_I^2+b^2)}$, with $b = \beta\sqrt{(T_0/(\rho c)}$, are the isothermal and adiabatic phase velocities (Rudgers 1990; Carcione *et al.* 2018). We see that the P wave propagation is dissipative because of the coupling of the bulk stresses with the heat-conduction equation. There are two longitudinal waves, an elastic E wave (a fast P wave) and a T wave (a slow thermal P wave). We have two real solutions for $\omega = 0$,

$$V_c = 0 \text{ (T wave)}, \quad V_c = V_A \text{(E wave)}. \quad (11)$$

For $c \to \infty$, we have $V_c = V_I$, whereas for $\gamma \to 0$, we obtain $V_c = V_A$. For $\gamma \to \infty$ or $\omega \to \infty$, V_c becomes the high-frequency limit E wave velocity $V_{E\infty}$ and limit T wave velocity $V_{T\infty}$, respectively. A detailed discussion on the values of τ associated with relaxation peaks and peak frequencies are given in Carcione *et al.* (2018).

3.2 Dispersion and attenuation behavior

The model with the thermoelastic properties, $\rho = 2600$ kg/m^3, $\lambda = 4$ GPa, $\mu = 6$ GPa, $T_0 = 318$ °K, $\alpha = 4.09\times10^{-6}$ °K^{-1}, and $c = 104$ m/(s^2°K). We consider two cases for the thermal conductivity, one with $\gamma = 2.61$ m kg/ (s^3°K) typical of rocks and the other with a higher value of $\gamma = 4.5\times10^4$ m kg/ (s^3°K) to illustrate the physics. The phase velocity $V_p = [\mathrm{Re}(1/V_c)]^{-1}$, and the attenuation coefficient $A_c = -4\pi\cdot\mathrm{Im}(1/V_c)\cdot V_p$ can be calculated from the complex velocity V_c, as a function of frequency (see Carcione 2014).

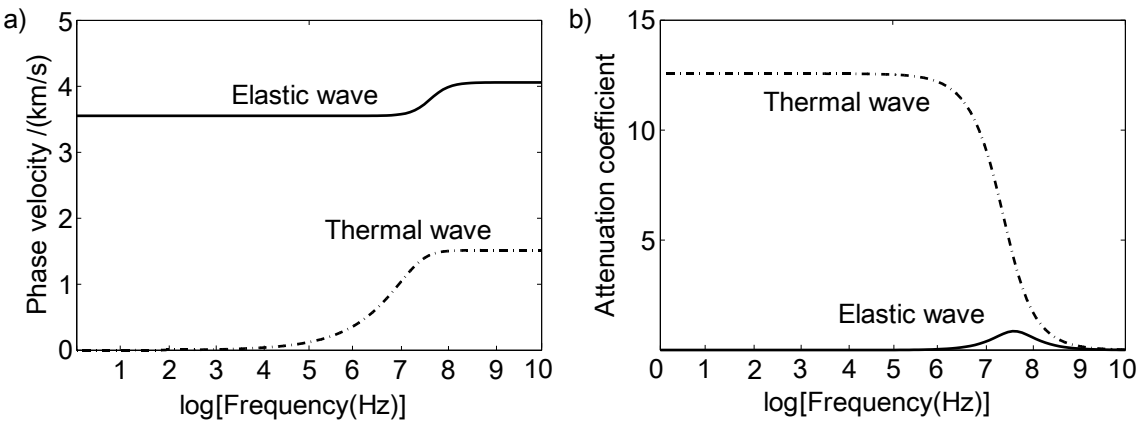

Figure 1. Phase velocities (a) and attenuation coefficients (b) of the E and T waves as a function of frequency for the thermal conductivity γ = 2.61 m kg/ (s^3°K).

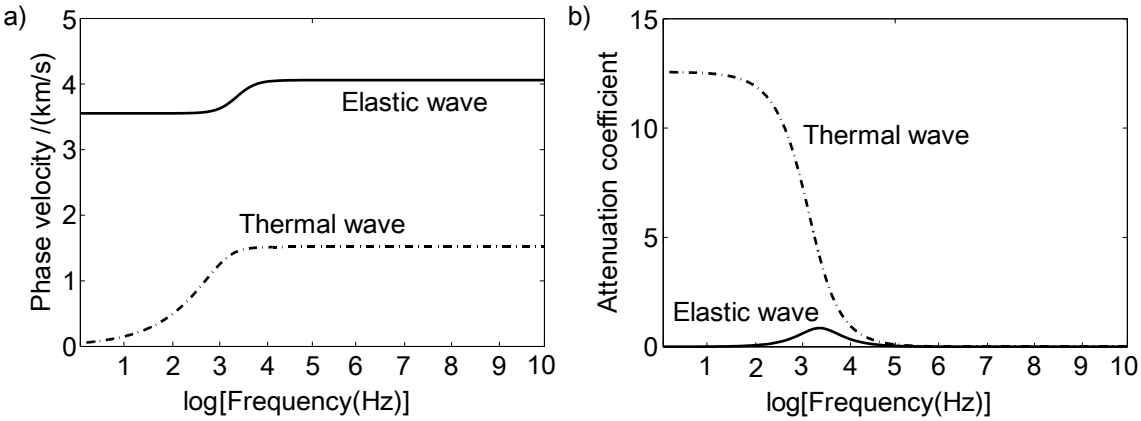

Figure 2. Phase velocities (a) and attenuation coefficients (b) of E and T waves as a function of frequency for the thermal conductivity $\gamma = 4.5\times10^4$ m kg/ (s^3°K).

Figures 1 and 2 show the phase velocities and attenuation coefficients of the elastic and thermal waves as a function of frequency for the two values of the thermal conductivity, respectively. The inflexion point of the velocity occurs at a frequency $f_p = V_I^2/(2\pi a^2)$, nearly at 39 MHz in the first case and 2.26 KHz in the second case. As can be seen, the E wave low frequency velocity is the adiabatic one, i.e., V_A = 3553 m/s, whereas V_I = 2481 m/s, the isothermal velocity, is not involved in the coupled case. The high-frequency E wave limit velocity is $V_{E\infty}$ = 4059 m/s, the high-frequency T wave limit velocity is $V_{T\infty}$ = 1516 m/s, close to the S wave velocity.

Because of the thermoelastic due to heat diffusion, the E and T waves are attenuated and undergo dispersion. Note that the attenuation coefficient of the two waves have a peak ($A_c \approx 1$), in both cases at the angular frequency $\omega \approx 1/\tau$, depending on the values of γ (Rudgers 1990). We obtain a peak at the ultrasonic band for values of γ typical of rocks. Increasing τ, the peak moves to low frequencies. The time scale for heat diffusion is a function of the length scale involved in the process of heat flow. The behavior of the T wave has similar characteristics to that of the Biot slow diffusive wave.

The mathematical analogy identifies temperature field in thermoelasticity with fluid pressure in poroelasticity (Bonnet 1987; Manolis & Beskos 1989; Norris 1991).

The thermal conductivity γ ranges from 24000 m kg/ (s^3°K) for CRC aluminum to 0.023 m kg/ (s^3°K) for air, whereas rocks filled with fluids have a range between 1 and 12 m kg/ (s^3°K). We select two very dissimilar values, namely $\gamma = 2.6$ m kg/ (s^3°K) and $\gamma = 4.5\times10^4$ m kg/ (s^3°K), to show how the physics behaves.

4 GREEN'S FUNCTIONS

Green's functions represent the fundamental solution to partial differential equations with a point source (the force or heat source). The Green function of the classical thermoelasticity theory (a parabolic-type equation) has been derived for a homogeneous isotropic medium (Tosaka & Suh 1991). In this section, we formulate the Green function of the modified thermoelasticity equations with a relaxation term (Lord & Shulman 1967). The derived process generally consists of three steps (e.g., Pao & Varatharajulu 1976): structuring the fundamental equation for the solution of partial differential equations to a point source, solving the fundamental equation by variables separation method, and reconstructing the fundamental solution tensor.

4.1 Fundamental equation

Applying the Fourier transform defined by

$$\tilde{u}(\mathbf{x},\omega) = \int_0^\infty u(\mathbf{x},t)\, e^{-i\omega t} dt, \tag{12}$$

to equation (5), we obtain the following differential equations in the frequency domain (omitting the hat for convenience):

$$\begin{cases} \mu u_{i,jj} + (\lambda+\mu) u_{j,ji} + \rho\omega^2 u_i - \beta T_{,i} = 0, \\ \gamma T_{,jj} - c(i\omega - \tau\omega^2) T - T_0 \beta (\mathrm{i}\omega - \tau\omega^2) u_{j,j} = 0. \end{cases} \tag{13}$$

It is convenient to rewrite the above system in the following matrix form:

$$L_{ij} U_j = 0, \tag{14}$$

where

$$L_{ij} = \begin{vmatrix} \mu\Delta + (\lambda+\mu) D_1^2 + \rho\omega^2 & (\lambda+\mu) D_1 D_2 & -\beta D_1 \\ (\lambda+\mu) D_1 D_2 & \mu\Delta + (\lambda+\mu) D_1^2 + \rho\omega^2 & -\beta D_2 \\ -T_0\beta(i\omega - \tau\omega^2) D_1 & -T_0\beta(i\omega - \tau\omega^2) D_2 & \gamma\Delta - \mathrm{c}(i\omega - \tau\omega^2) \end{vmatrix},$$

and

$$U_j = < \tilde{u}_1 \ \ \tilde{u}_2 \ \ \tilde{T} >,$$

with the notation $D_i = \partial/\partial x_i$ (i = 1,2).

The fundamental solution tensor (a weighting tensor as the basic components of Green's function) V_{ij}^* satisfies the differential equation to a point source,

$$L_{ij}^* V_{jk}^* = -\delta_{ik}^* \delta(x-y), \tag{15}$$

where L_{ij}^* is the adjoint cofactor operator of L_{ij}.

$$L_{ij}^* = \begin{vmatrix} \mu\Delta + (\lambda+\mu)D_1^2 + \rho\omega^2 & (\lambda+\mu)D_1 D_2 & -T_0\beta(\mathrm{i}\omega - \tau\omega^2)D_1 \\ (\lambda+\mu)D_1 D_2 & \mu\Delta + (\lambda+\mu)D_1^2 + \rho\omega^2 & -T_0\beta(\mathrm{i}\omega - \tau\omega^2)D_2 \\ -\beta D_1 & -\beta D_2 & \gamma\Delta - \mathrm{c}(\mathrm{i}\omega - \tau\omega^2) \end{vmatrix}$$

4.2 Fundamental solutions

In order to derive the solution to equation (15), we follow Kupradze *et al*. (1979) and Tosaka & Suh (1991) and make use of the fundamental solution tensor V_{ij}^* in terms of the scalar potential function Φ^* and the transposed co-factor operator L_{ij}^{T} of L_{ij}^*.

$$V_{ij}^*(x,y,s) = L_{ij}^T \Phi^*(x,y,s). \tag{16}$$

Substitution of equation (16) into (15) yields

$$\Lambda\Phi^* = -\delta(x-y), \tag{17}$$

where

$$\Lambda = \det\left(L_{ij}^*\right) = \frac{\mu}{\lambda+2\mu}(\Delta - h_1^2)(\Delta - h_2^2)(\Delta - h_3^2), \tag{18}$$

and the coefficient of h_i^2 can be determined as these which satisfy

$$\begin{cases} h_1^2 + h_2^2 = \dfrac{\rho\omega^2}{\lambda+2\mu} - \dfrac{\mathrm{i}\omega(1+\mathrm{i}\omega\tau)}{\kappa}\left(1 + \dfrac{\beta^2 T_0}{c(\lambda+2\mu)}\right), \\ h_1^2 h_2^2 = -\dfrac{\rho\omega^2}{\lambda+2\mu} \cdot \dfrac{\mathrm{i}\omega(1+\mathrm{i}\omega\tau)}{\kappa}, \\ h_3^2 = \dfrac{\rho\omega^2}{\mu}. \end{cases} \tag{19}$$

Note that h_1 and h_2 are functions of the relaxation time τ, while, h_3 and τ are not related.

Using equation (18), the fundamental solution for Φ^* from equation (17) can be formulated as

$$\Phi^* = \frac{\lambda + 2\mu}{2\pi\mu} \sum_{i=1}^{3} W_i K_0(\mathrm{i}h_i r), \tag{20}$$

where

$$W_i = \frac{-1}{(h_i^2 - h_j^2)(h_k^2 - h_i^2)} \; (i = 1,2,3 \; j = 2,3,1 \; k = 3,1,2). \tag{21}$$

Each component of the fundamental solution tensor V_{ij}^* can be obtained by employing the derived fundamental solution as follows:

$$\begin{cases} V_{ij}^* = \dfrac{1}{2\pi\mu} W_k \displaystyle\sum_{k=1}^{3} \left(\psi_k(r)\delta_{ij} - \chi_k(r) r_{,i} r_{,j}\right), (i,j = 1,2), \\ V_{3i}^* = \dfrac{\beta}{2\pi(\lambda + 2\mu)} \displaystyle\sum_{k=1}^{3} W_k \xi_k(r) r_{,i}, (i = 1,2), \\ V_{i3}^* = \dfrac{\mathrm{i}\omega\eta}{2\pi(\lambda + 2\mu)} \displaystyle\sum_{k=1}^{3} W_k \xi_k(r) r_{,i}, (i = 1,2), \\ V_{33}^* = \dfrac{1}{2\pi} \displaystyle\sum_{k=1}^{3} W_k \zeta_k(r), \end{cases} \tag{22}$$

where

$$\begin{cases} \psi_k(r) = \left[(h_k^2 + m)(h_k^2 - m_1) + \dfrac{\eta\beta\kappa m h_k^2}{\lambda + 2\mu}\right] K_0(\mathrm{i}h_k r) - P_k \dfrac{h_k}{r} K_1(\mathrm{i}h_k r), \\ \chi_k(r) = P_k h_k^2 K_2(\mathrm{i}h_k r), \\ \xi_k(r) = -(h_k^2 - m_2)\mathrm{i}h_k K_1(\mathrm{i}h_k r), \\ \zeta_k(r) = (h_k^2 - m_1)(h_k^2 - m_2) K_0(\mathrm{i}h_k r), \end{cases} \tag{23}$$

with

$$P_k = \frac{\lambda + \mu}{\lambda + 2\mu}(h_k^2 + m), \tag{24}$$

and

$$m = \frac{\mathrm{i}\omega(1 + \mathrm{i}\omega\tau)}{\kappa}, m_1 = \frac{\rho\omega^2}{\lambda + 2\mu}, m_2 = \frac{\rho\omega^2}{\mu}, \kappa = \frac{\gamma}{c}, \eta = \frac{\beta T_0}{\gamma}. \tag{25}$$

Here, K_0, K_1, K_2 are the modified Bessel function of the second kind of order zero, first, and second, respectively, with the argument $r = \| x - y \|$.

To understand the physical meaning of the basic components of the Green function (i.e., fundamental solution tensor), it is convenient to write the fundamental solution in matrix form as

$$V_{ij}^{*} = \begin{vmatrix} V_{11}^{*} & V_{12}^{*} & V_{13}^{*} \\ V_{21}^{*} & V_{22}^{*} & V_{23}^{*} \\ V_{31}^{*} & V_{32}^{*} & V_{33}^{*} \end{vmatrix}. \qquad (26)$$

This Green function is a second-order tensor with nine components, where (V_{11}^{*}, V_{21}^{*}, V_{31}^{*}), (V_{12}^{*}, V_{22}^{*}, V_{32}^{*}) and (V_{13}^{*}, V_{23}^{*}, V_{33}^{*}) correspond to the horizontal particle velocity, vertical particle velocity and temperature, respectively, of a horizontal elastic force, a vertical elastic force, and a heat source, respectively.

4.3 Numerical experiments

We use the analytical method, based on the proposed second-order tensor Green's function [equation (22)], to calculate wavefield snapshots, where the model parameters are consistent with those used in Carcione *et al.* (2018). The source is a vertical force and has the time function $h(t) = \cos[(t - t_0)\, f_0] \cdot \exp[-2(t - t_0)^2 f_0^2]$, where the central frequency is f_0 = 3.5 MHz and $t_0 = 3/(2f_0)$ is a delay time.

Figure 3 shows the vertical particle velocity (a) and temperature field (b) for a heat source, with γ = 10.5 m kg/ (s^3°K). As expected, there is no S wave. The velocity of the E wave is slightly less than $V_{E\infty}$, whereas the T wave is diffusive. As predicted by Figure 1(b), the T wave is highly attenuated and can hardly be seen.

Figure 4 shows the vertical particle velocity (a) and temperature field (b) for a heat source, corresponding to $\gamma = 4.5\times10^6$ m kg/ (s^3°K). The E and T wavefronts travel with the velocities $V_{E\infty}$ and $V_{T\infty}$, respectively. The difference with Figure 3 is the weak attenuation of the T wave, in agreement with Figure 2(b).

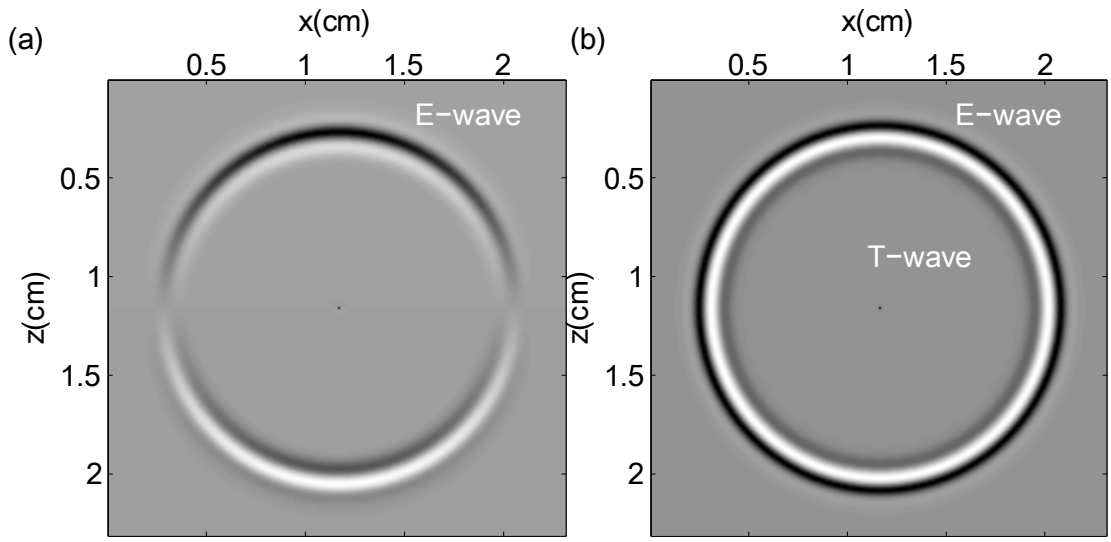

Figure 3. Snapshots of the vertical component of the particle velocity (a) and temperature (b) at 3 μs,

corresponding to the coupled case with γ = 10.5 m kg/ (s^3°K). The perturbation is a heat source with a central frequency of 3.5 MHz.

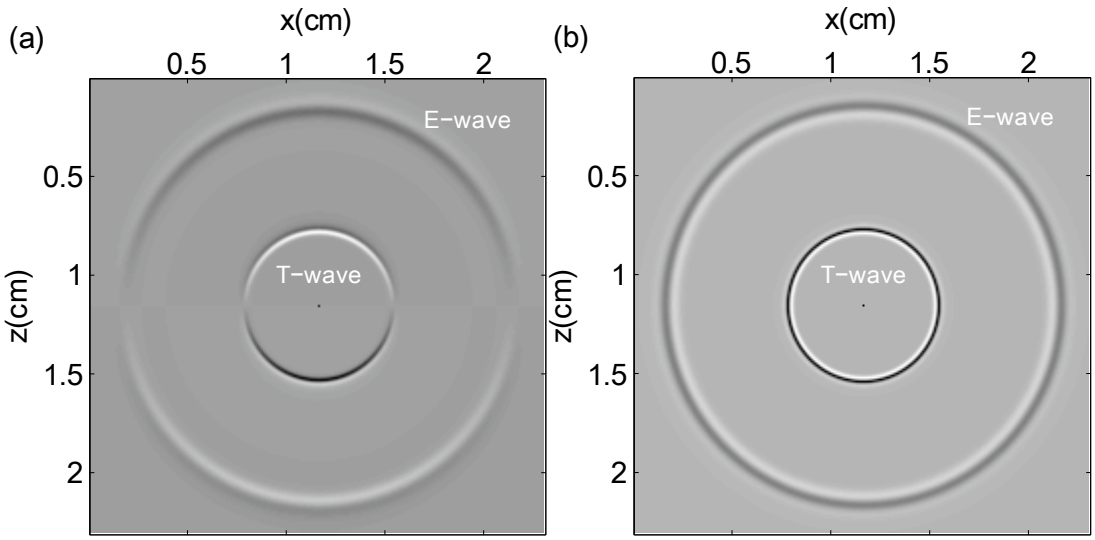

Figure 4. Snapshots of the vertical component of the particle velocity (a) and temperature (b) at 3 μs, corresponding to the coupled case with a high thermal conductivity of $\gamma = 4.5\times10^6$ m kg/(s^3°K). The perturbation is a heat source with a central frequency of 3.5 MHz.

To compare snapshots generated by the elastic and heat sources, we consider a 231×231 mesh with square cells and a grid spacing of $dx = dz$ = 100 μm. The source is a Ricker wavelet located at the center of the mesh with f_0 = 1.5 MHz. The model thermoelastic properties are same as those in the section 3.2. Figure 5 shows snapshots of the horizontal particle velocity (left panel), vertical particle velocity (middle panel), and temperature (right panel) are calculated at 2.6 μs according to equation (26), with γ = 2.61 m kg/ (s^3°K), for a horizontal elastic force (a), a vertical elastic force (b), and a heat source (c). The E (i.e., fast P wave) and S wave have their motions consistent with the radiation pattern for point forces (Aki & Richards 2002). The velocity of the E wave is slightly less than $V_{E\infty}$. The T wave is highly attenuated according to Figure 1(b).

(a) horizontal elastic force

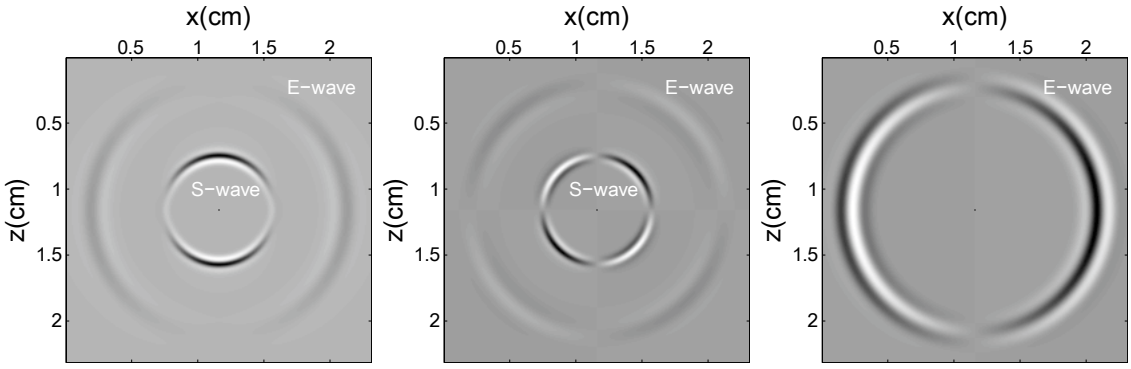

(b) vertical elastic force

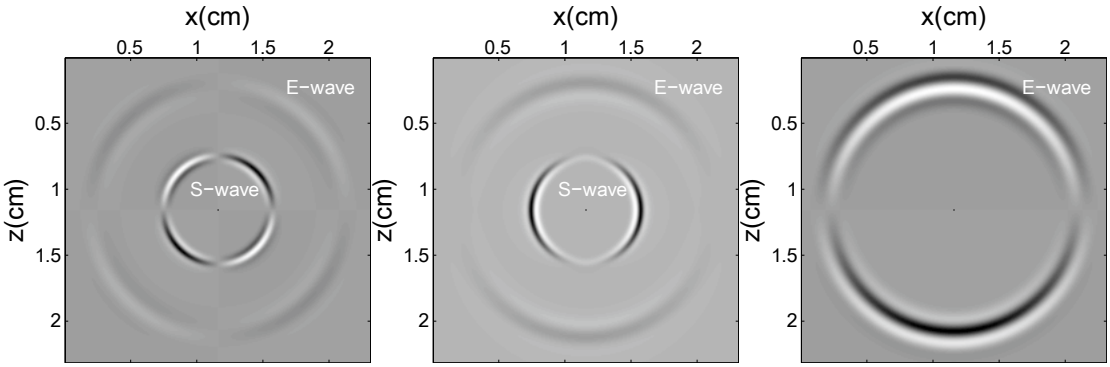

(c) heat force

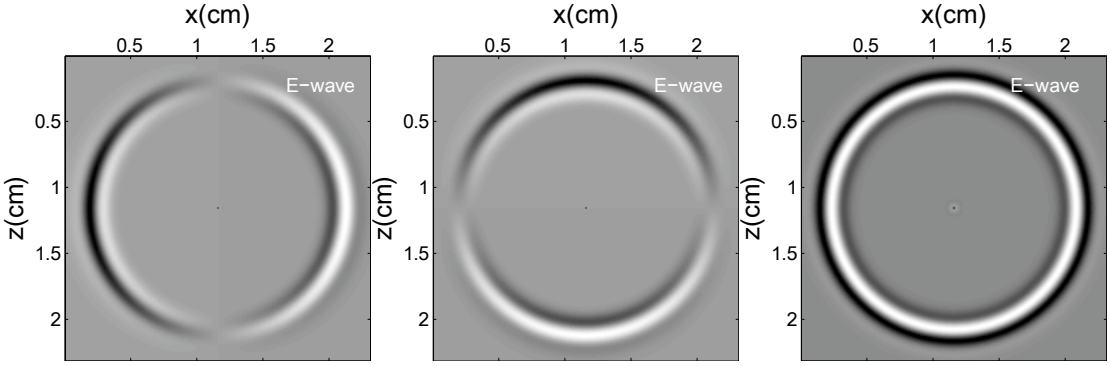

Horizontal particle velocity Vertical particle velocity Temperature

Figure 5. Snapshots of the horizontal particle velocity (left panel), vertical particle velocity (middle panel), and temperature (right panel) at 2.6 μs, calculated for a thermal conductivity of γ = 2.61 m kg/ (s^3°K), with a horizontal elastic force (a), a vertical elastic force (b), and a heat source (c), corresponding to a Ricker-wavelet frequency of f_0 = 1.5 MHz.

Figure 6 shows snapshots of the particle velocity and temperature tensor for γ = 4.5×10^4 m kg/ (s^3°K) along the *x*- and *z*- directions for a Ricker wavelet frequency of f_0 = 1.5 MHz. The snapshots of the horizontal particle velocity (left panel), vertical particle velocity (middle panel), and temperature (right panel) are calculated at 2.6 μs, according to equation (26), for a horizontal elastic force (a), a vertical elastic force (b), and a heat source (c). The E and S waves have their motions consistent with the radiation pattern for point forces (Aki & Richards 2002). The E and T wavefronts travel with the velocities $V_{E\infty}$ and $V_{T\infty}$. We can see the T wave, since the attenuation is negligible, in agreement with Figure 2(b).

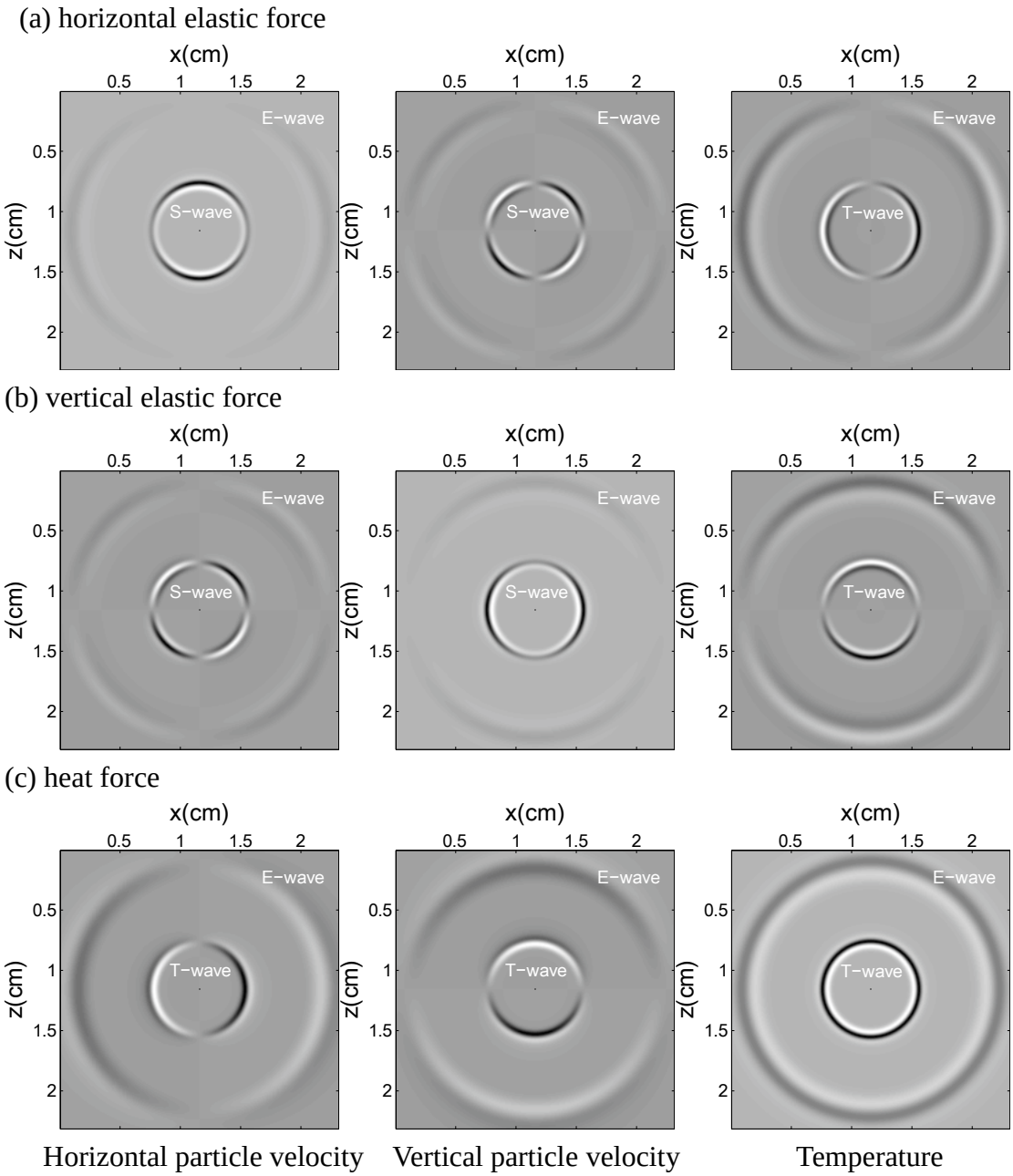

Figure 6. Snapshots of the horizontal particle velocity (left panel), vertical particle velocity (middle panel), and temperature (right panel) at 2.6 μs, calculated with the thermal conductivity $\gamma = 4.5\times10^4$ m kg/ (s^3°K), for a horizontal elastic force (a), a vertical elastic force (b), and a heat source (c) corresponding to a Ricker-wavelet frequency of f_0 = 1.5 MHz.

5 CONCLUSIONS

We have considered the modified thermoelasticity equations that incorporate a relaxation term to overcome the unphysical behavior described by the classical theory. We formulate a second-order tensor Green's function for wave propagation in a homogeneous isotropic medium. It is the displacement-temperature solution to a point

(elastic or heat) source. The Green function is generally used as the fundamental solution for the integral equation representation of thermoelasticity problems and a test of numerical algorithms. The theory predicts three distinct waves, an E wave (a fast P wave), a T wave (a thermal P wave), and an S wave (a shear wave). The P waves suffer attenuation and velocity dispersion because of the compression/expansion-induced temperature gradients leading to mechanical energy dissipation and heat conduction, where the S wave is unaffected by the thermal effects.

We compare the heat-source induced wavefield snapshots of the vertical particle velocity and temperature by assuming a very high thermal conductivity with a smaller one typical of rocks. In the latter case, the T wave has a diffusive character, whereas it is wave-like for a much higher conductivity. For a heat source, there are no S waves. We also compare snapshots of the horizontal/vertical particle velocities and temperature generated by horizontal/vertical elastic forces and heat source. These numerical experiments show that the elastic and thermal P modes are dispersive and lossy, as predicted by the plane-wave analyses. These modes have similar characteristics of the fast and slow P waves of the poroelasticity theory. In particular, the thermal mode is diffusive at low thermal conductivities and becomes wave-like for high thermal conductivities. In poroelasticity, this corresponds to high and low fluid viscosities.

A detailed account of the boundary integral equation formulation and implementation by boundary-element numerical methods using the Green function presented here will be the subject of a future paper.

ACKNOWLEDGMENTS

Valuable comments by Rene-Edouard Plessix, Sven Treitel and anonymous reviewer significantly improved the paper. The work presented here was supported by the Major State Research Development Program of China (Grant no. 2016YFC0601101) and the Chinese Academy of Sciences Strategic Leading Science and Technology projects (Grant no. XDA10010403), and PetroluemChina Project (Grant no. 2016A-4801).

Appendix A. List of symbols

u_i	components of the displacement (i = 1, 2, 3)
ϵ_{ij}	strain components (i, j = 1, 2, 3)
σ_{ij}	stress components (i, j = 1, 2, 3)
λ, μ	Lamé constants
δ_{ij}	Kronecker-delta component
f_{ij}	external stress forces (i, j = 1, 2, 3)
T_0	absolute temperature for the state of zero stress and strain
T	increment of temperature above a reference absolute temperature T_0
α	coefficient of thermal expansion
β	stress-temperature modulus
f_i	components of the external body forces (i = 1, 2, 3)
ρ	mass density
γ	coefficient of heat conduction (or thermal conductivity)
c	specific heat of the unit volume in the absence of deformation
τ	relaxation time
q	heat source
Δ	Laplacian operator
ω	angular frequency
V_c	complex velocity
s	slowness
d_i	directions of the displacement vector (i = 1, 2, 3)
x_i	position components (i = 1, 2, 3)
l_i	the propagation direction (i = 1, 2, 3)
A, B	amplitude constants
a	thermal diffusivity
V_I	isothermal phase velocities
V_A	adiabatic phase velocities

subscript ‘,i’ denotes a spatial derivative.

Appendix B. Velocity of the S and P waves in a homogenous thermoelastic medium

To derive the P and S wave velocities, we use equation (6) to obtain the following functions related to displacement and temperature,

$$\begin{cases} u_{i,jj} = -\left(\frac{\omega}{V_c}\right)^2 Ad_i, u_{j,ji} = -\left(\frac{\omega}{V_c}\right)^2 Ad_j l_j l_i, \ddot{u}_i = -\omega^2 Ad_i, \\ T_{,jj} = -\left(\frac{\omega}{V_c}\right)^2 B, \ddot{u}_{j,j} = \mathrm{i}\frac{\omega}{V_c}\omega^2 Ad_j l_j, \dot{u}_{j,j} = \frac{\omega}{V_c}\omega Ad_j l_j, \\ T_{,i} = -\mathrm{i}\frac{\omega}{V_c} Bl_i, \dot{T} = \mathrm{i}\omega B, \ddot{T} = -\omega^2 B, \end{cases} \quad \text{(B-1)}$$

where the exponential term is omitted for the sake of brevity. Substituting equation (B-1) into (5), we obtain a system of algebraic equations

$$\begin{cases} \mu\left(\frac{\omega}{V_c}\right)^2 Ad_i - \rho\omega^2 Ad_i + (\lambda+\mu)\left(\frac{\omega}{V_c}\right)^2 Ad_j l_j l_i - \mathrm{i}\gamma B\beta l_i = 0, \\ c(\mathrm{i}\omega B - \tau\omega^2 B) + T_0\beta\left(\frac{\omega}{V_c}\omega Ad_j l_j + \mathrm{i}\tau\frac{\omega}{V_c}\omega^2 Ad_j l_j\right) + \gamma\left(\frac{\omega}{V_c}\right)^2 B = 0. \end{cases} \quad \text{(B-2)}$$

For the S wave, $d_i\, l_i = 0$ and equation (B-2) reduces to

$$\begin{cases} \left[\mu\left(\frac{\omega}{V_c}\right)^2 - \rho\omega^2\right] A - \mathrm{i}\frac{\omega}{V_c}\beta B = 0, \\ \left[\mathrm{i}\omega c - \omega^2\tau + \gamma\left(\frac{\omega}{V_c}\right)^2\right] B = 0. \end{cases} \quad \text{(B-3)}$$

The solution to this equation for the S wave velocity is

$$B = 0, V_c = \sqrt{\mu/\rho}. \quad \text{(B-4)}$$

For the P wave, $d_i\, l_i = 1$ and equation (B-2) reduces to

$$\begin{cases} \left[-\rho\omega^2 + (\lambda+2\mu)\left(\frac{\omega}{V_c}\right)^2\right] A = \mathrm{i}\beta\frac{\omega}{V_c} B, \\ \mathrm{i}\beta T_0\frac{\omega}{V_c}(\mathrm{i}\omega - \tau\omega^2) A = \left(\mathrm{i}c\omega + \gamma\left(\frac{\omega}{V_c}\right)^2 - c\tau\omega^2\right) B. \end{cases} \quad \text{(B-5)}$$

Eliminating the constants A and B leads to the secular equation

$$\left[-\rho\omega^2 + (\lambda+2\mu)\left(\frac{\omega}{V_c}\right)^2\right]\left[\mathrm{i}c\omega + \gamma\left(\frac{\omega}{V_c}\right)^2 - c\tau\omega^2\right] = -\beta^2\gamma\, T_0\frac{\omega}{V_c}(\mathrm{i}\omega - \tau\omega^2). \quad \text{(B-6)}$$

By introducing the variables $a = \sqrt{(\gamma/c)}$, $b = \beta\sqrt{(T_0/(\rho c)}$ and $V_I = \sqrt{((\lambda+2\mu)/\rho)}$, $V_A =$

$\sqrt{(V_I^2+b^2)}$, we have

$$(-V_c^2 + V_A^2)i\omega(1 + i\tau\omega) + [-V_c^2 + V_I^2]a^2\left(\frac{\omega}{V_c}\right)^2 = 0. \quad \text{(B-7)}$$

Defining $M = (i\omega a^2)/(1+i\tau\omega)$, equation (B-7) can be further written as

$$V_c^4 - (V_A^2 + M)V_c^2 + V_I^2 M = 0. \quad \text{(B-8)}$$

The solution to this equation for the P wave velocity is

$$2V_c^2 = V_A^2 + M \pm \sqrt{(V_A^2 + M)^2 - 4V_I^2 M}. \quad \text{(B-9)}$$

REFERENCES

Ackerman, C. C., Bertman, B., Fairbank, H. A. & Guyer, R. A., 1966. Second sound in solid helium, *Physical Review Letters*, **16**, 789.

Aki, K. & Richards, P. G. 2002. *Quantitative Seismology*, 2nd Ed: University Science Books,U.S.

Armstrong, B. H., 1984. Models for thermoelastic attenuation of waves in heterogeneous solids, *Geophysics*, **49**, 1032-1040.

Auriault, J. L., 2014. Inner thermal resonance in thermoelastic geological structures, *Acta Geophysica*, **62**, 993-1004.

Banerjee, D. K. & Pao, Y. H., 1974. Thermoelastic waves in anisotropic solids, *Journal of the Acoustical Society of America*, **56**, 1444-1454.

Bear, J., Sorek, S., Ben-Dor, G. & Mazor, G., 1992. Displacement waves in saturated thermoelastic porous media. I. Basic equations, *Fluid dynamics research*, **9**, 155-164.

Biot, M. A., 1956. Thermoelasticity and irreversible thermodynamics, *Journal of Applied Physics*, **27**, 240-253.

Bonnet, G., 1987. Basic singular solutions for a poroelastic medium in the dynamic range, *Journal of the Acoustical Society of America*, **82**, 1758-1762.

Boschi, E., 1973. A thermoviscoelastic model of the earthquake source mechanism, *Journal of Geophysical Research*, **78**, 7733-7737.

Carcione, J. M., 2014. *Wave fields in real media: Wave propagation in anisotropic, anelastic, porous and electromagnetic media*, Elsevier.

Carcione, J. M., Cavallini, F., Wang, E., Ba, J. & Fu, L.Y., 2019. Simulation of wave propagation in linear thermo-poroelastic media, *Journal of Geophysical Research*,

in press.

Carcione, J. M., Wang, Z. W., Ling, W., Salusti, E., Ba, J. & Fu, L.Y., 2018. Simulation of wave propagation in linear thermoelastic media, *Geophysics*, **84**, T1-T11.

Chandrasekharaiah, D. S., 1998. Hyperbolic thermoelasticity: a review of recent literature, *Applied Mechanics Reviews*, **51**, 705-729.

Deresiewicz, H., 1957. Plane waves in a thermoelastic solid, *Journal of the Acoustical Society of America*, **29**, 204-209.

Hetnarski, R. B. & Ignaczak, J., 1997. On solition-like thermoelastic waves, *Applicable Analysis*, **65**, 183-204.

Hetnarski, R. B., & Ignaczak, J., 1999. Generalized thermoelasticity, *Journal of Thermal Stresses*, **22**, 451-476.

Hörmander L., 2013. *Linear partial differential operators*, Springer.

Jackson, H. E., Walker, C. T. & McNelly, T. F., 1970. Second sound in NaF, *Physical Review Letters*, **25**, 26.

Jacquey, A. B., Cacace, M., Blöcher, G. & Scheck-Wenderoth, M., 2015. Numerical investigation of thermoelastic effects on fault slip tendency during injection and production of geothermal fluids, *Energy Procedia*, **76**, 311-320.

Ignaczak, J. & Ostoja-Starzewski M., 2010. *Thermoelasticity with finite wave speeds*, Oxford University Press.

Green, A. E. & Lindsay, K. A., 1972. Thermoelasticity, *Journal of elasticity*, **2**, 1-7.

Green, A. E. & Naghdi, P. M., 1993. Thermoelasticity without energy dissipation, *Journal of elasticity*, **31**, 189-208.

Kupradze, V. D., Gegelia, T. G., Basheleishvili, M. O. & Burchuladze, T. V., 1976. *Three-dimensional problems of the mathematical theory of elasticity and thermoelasticity*, North-Holland.

Lord, H. W. & Shulman, Y., 1967. A generalized dynamical theory of thermoelasticity, *Journal of the Mechanics and Physics of Solids*, **15**, 299-309.

Manolis, G. D. & Beskos, D. E., 1989. Integral formulation and fundamental solutions of dynamic poroelasticity and thermoelasticity, *Acta Mechanica*, **76**, 89-104.

McNelly, T. F., Rogers, S. J., Channin, D. J., Rollefson, R. J., Goubau, W. M., Schmidt, G. E. & Pohl, R. O., 1970. Heat pulses in NaF: onset of second sound, *Physical Review Letters*, **24**, 100.

Nowacki, W., 1975. *Dynamic problems of thermoelasticity*, Springer Science & Business Media.

Norris, A. N., 1991. On the correspondence between poroelasticity and thermoelasticity, *Journal of Applied Physics*. **71**, 1138-1141.

Norris, A. N., 1994. Dynamic Green's functions in anisotropic piezoelectric, thermoelastic and poroelastic solids, Proceedings of the Royal Society A: Mathematical, *Physical and Engineering Sciences*, **447**, 175-188.

Pao, Y. H. & Varatharajulu, V., 1976. Huygens' principle, radiation conditions, and integral formulas for the scattering of elastic waves, *Journal of the Acoustical Society of America*, **59**, 1361–1370.

Rudgers, A. J., 1990. Analysis of thermoacoustic wave propagation in elastic media, *Journal of the Acoustical Society of America*, **88**, 1078-1094.

Sharma, M. D., 2008. Wave propagation in thermoelastic saturated porous medium, *Journal of Earth System Science*, **117**, 951-958.

Savage, J. C., 1966. Thermoelastic Attenuation of Elastic Waves by Cracks, *Journal of Geophysical Research*, **71**, 3929-3938.

Tosaka, N., 1985. The integral equation formulation for boundary-value problems by the coupled system of differential equations (in Japanese), *Japan NCTAM*, 323–324.

Tosaka, N. & Suh, I. G., 1991. Boundary element analysis of dynamic coupled thermoelasticity problems, *Computational mechanics*, **8**, 331-342.

Treitel, S., 1959. On the Attenuation of Small-Amplitude Plane Stress Waves in a Thermoelastic Solid, *Journal of Geophysical Research*, **64**, 661-665.

Tsai, V. C., 2011. A model for seasonal changes in GPS positions and seismic wave speeds due to thermoelastic and hydrologic variations, *Journal of Geophysical Research*, **116**.

Turchetti, G. & Mainardi, F., 1976. Wave front expansions and Padé approximants for transient waves in linear dispersive media, *In Padé Approximants Method and Its Applications to Mechanics*. Springer, Berlin, Heidelberg, 189-207.

Tzou, D. Y., 1995. A unified field approach for heat conduction from macro-to micro-scales, *Journal of Heat Transfer*, **117**, 8-16.

Vernotte, P., 1948. Théorie continue et théorie moléculaire des phénomènes thermocinétiques, *Comptes rendus de l'Académie des Sciences*, **227**, 43–44.

Zener, C., 1938. Internal friction in solids II. General theory of thermoelastic internal friction, *Physical Review*, **53**, 90-99.